Energy-conserving, Implicit PIC Algorithms for electric propulsion and plasma plumes

Pedro Jimenez, Mario Merino

31st Spacecraft Plasma Interaction Network in Europe (SPINE) meeting October 2024
Toulouse

Why are Fast and Accurate Kinetic Models needed in Spacecraft-Plasma Interactions studies?

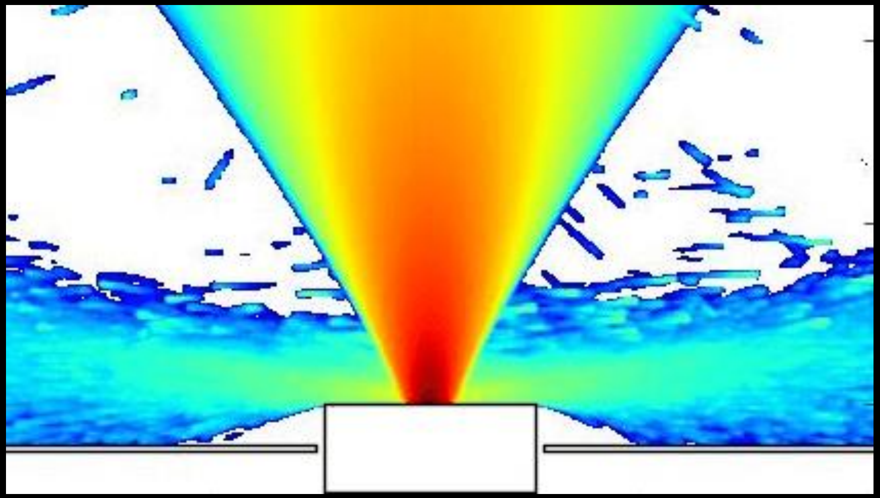

- Predictive Accuracy:
  - Spacecraft interact with diverse plasma environments, affecting performance and safety.
  - Kinetic models can predict **charging**, **erosion** more accurately than alternatives.
  - Low density and weakly collisional plasmas.
    - Lack of thermodynamics equilibrium.
- Particle-in-Cell has become the most popular method for large scale kinetic simulations
- An important numerical parameter is the number of macroparticles per cell.
  - Should be large for statistical representation.
  - Classic models (explicit) must use fine meshes -> Many particles.
    - Long compute times.
- Implicit methods can use much course meshes and long time steps
  - Many less particles.

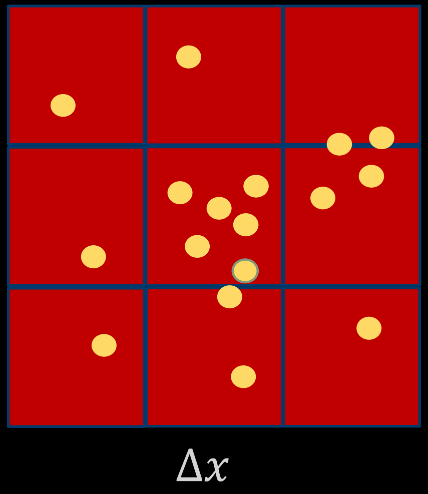

Electrodeless Thrusters (EPTs) and Magnetic Nozzles (MN)

- Electromagnetic (EM) waves heat the plasma. Magnetic nozzles used as the acceleration stage. Diverging $\boldsymbol{B}_a$ created by coils or magnets.

- Partial understanding of important mechanisms from fluid models:
  - Quasineutral and ambipolar expansion.
  - Different parametric regions for EM wave propagation.
  - Different heating mechanisms. Resonant (Electron Cyclotron Thruster ECRT), geometric-inductive (Helicon Plasma Thruster HPT).
  - Thermal electron energy to ion kinetic energy conversion in nozzle topology.

- However, lack local thermodynamic equilibrium and kinetic effects:
  - Electron kinetics, subpopulations and cooling .
  - Plasma wave-interaction and effects on EVDF not well understood.
  - Need for **accurate and fast** kinetic simulations.
    - **Implicit PIC** surpasses the performance of classical methods.

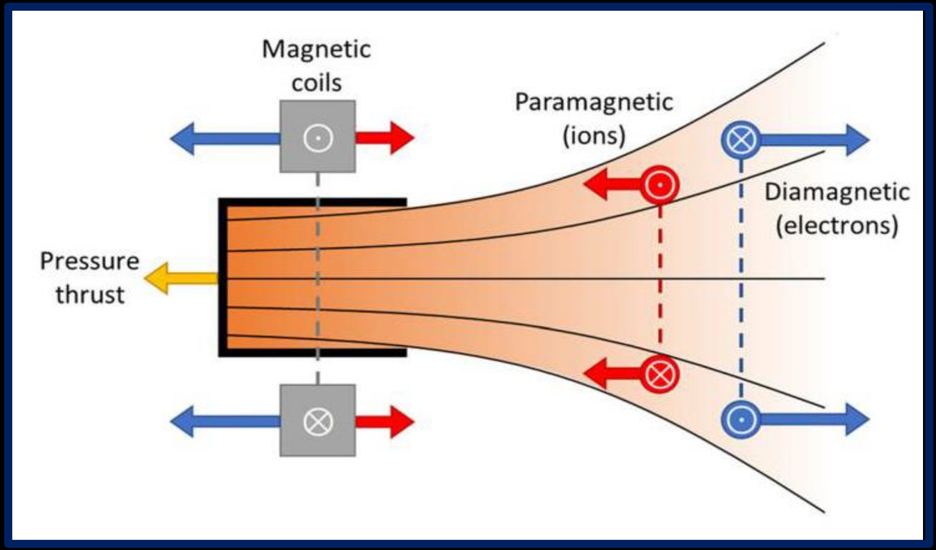

Governing Particle Equations

$$\frac{\partial f_s}{\partial t} + \frac{1}{B(\mathbf{x})}\left[\nabla\cdot(v_\parallel \mathbf{B} f_s) + \frac{\partial}{\partial v_\parallel}\left(\left(\frac{q_s}{m_s}E_\parallel - \tilde{\mu}\mathbf{b}\cdot\nabla B\right) B f_s\right)\right] = 0$$

$$f_s(z, v_z, \tilde{\mu}, t) = \sum_{p\in s} w_p \delta(z - z_p(t))\delta(v_z - v_{z,p}(t))\delta(\tilde{\mu} - \tilde{\mu}_p(t))$$

$$v_\parallel \approx v_z \;;\; E_\parallel \approx E_z \;;\; \mathbf{B} \approx B(z)\mathbf{z}\;; R\frac{\partial \ln B_{z0}}{\partial z} = \varepsilon \ll 1.$$

- Drift-kinetic Vlasov equation (DKE). Perpendicular drifts can be neglected by virtue of the Paraxial approximation.
- Particle discretization of the EDFs.
- Paraxial approximation and magnetized particles.

$$\frac{\ell_s}{R} \le O(\varepsilon),$$

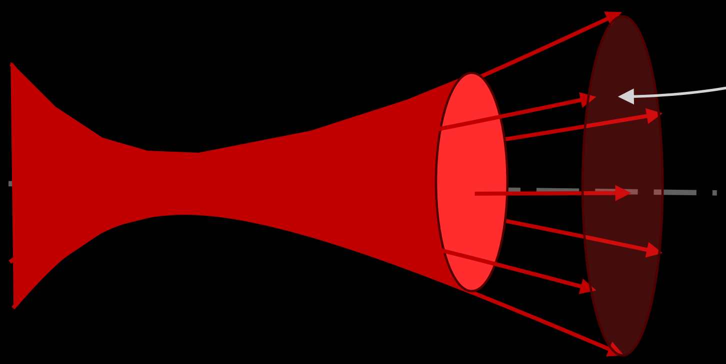

$$\begin{aligned}
\frac{\mathrm{d}z_p}{\mathrm{d}t} &= v_{z,p},\\
\frac{\mathrm{d}v_{z,p}}{\mathrm{d}t} &= \frac{q_s}{m_s}\left(E_z + v_{xp}B_y - v_y B_x\right) - \frac{1}{2B_{z0}}\frac{\partial B_{z0}}{\partial z}\left(v_{xp}^2 + v_{yp}^2\right),\\
\frac{\mathrm{d}v_{xp}}{\mathrm{d}t} &= \frac{q_s}{m_s}\left(E_x + v_{yp}B_{z0} - v_{zp}B_y\right) + \frac{1}{2B_{z0}}\frac{\partial B_{z0}}{\partial z}v_{zp}v_{xp},\\
\frac{\mathrm{d}v_{yp}}{\mathrm{d}t} &= \frac{q_s}{m_s}\left(E_y - v_{xp}B_{z0} + v_{zp}B_x\right) + \frac{1}{2B_{z0}}\frac{\partial B_{z0}}{\partial z}v_{zp}v_{yp}.
\end{aligned}$$

- **ES case**: Applied B_{z0} and ambipolar E_z only.
- **EM case**: Adds wave fields B_x, B_y and E_x, E_y
- **IW case:** EM fields from cold-plasma dielectric tensor model

- Evolution equations for the particles. 1D3V system.
  - Magnetic mirror force term.
- 1D1V if μ is assumed constant (only electrostatic).

Self-Consistent Field Equations: The Darwin Approximation

- Scalar and vector potentials (Coulomb's gauge) and wave equation:

$$\boldsymbol{E}_i = -\nabla\phi; \qquad \boldsymbol{E}_s = -\frac{\partial \boldsymbol{A}}{\partial t}; \qquad \boldsymbol{B}_s = \nabla \times \boldsymbol{A}.$$

$$\nabla \cdot E_i = \frac{\rho}{\varepsilon_0};$$

$$\nabla \times \boldsymbol{B}_s = \mu_0 \varepsilon_0 \frac{\partial(\boldsymbol{E}_i + \boldsymbol{E}_s)}{\partial t} + \mu_0 \boldsymbol{j}.$$

$$-\nabla^2 \phi = \frac{\rho}{\varepsilon_0};$$

$$-\nabla^2 \boldsymbol{A} = -\mu_0 \varepsilon_0 \left(\frac{\partial \nabla \phi}{\partial t} + \frac{\partial^2 \boldsymbol{A}}{\partial t^2} \right) + \mu_0 \boldsymbol{j}.$$

- Decoupled axial and transverse fields:

Paraxial factor

$$J^B = \frac{1}{B}$$

In 1D, we ignore A_z

$$\epsilon_0 \frac{\partial}{\partial t} \frac{\partial}{\partial z} \left(J^B \frac{\partial \phi}{\partial z} \right) = \frac{\partial (J^B j_z)}{\partial z},$$

$$\frac{\partial}{\partial z} \left(J^B \frac{\partial A_x}{\partial z} \right) = -\mu_0 J^B j_x,$$

$$\frac{\partial}{\partial z} \left(J^B \frac{\partial A_y}{\partial z} \right) = -\mu_0 J^B j_y.$$

- Hyperbolic Maxwell -> Elliptic Darwin
  - No CFL condition for speed of light (vacuum light waves are removed)
  - Darwin is a very good approx. in dense plasmas

Imposed Wave: Cold Plasma Dielectric Tensor Model

- Alternative, cold-plasma model to find E_x, E_y and impose the wave to the move particles. 1D equation for a right-hand circularly polarized wave
  - Frequency domain and not-self consistent with particle weighted currents.
  - Retains all terms in Maxwell's equations.
  - Phenomenological damping term γ.
- Employed in the past for full thruster 2D simulations

$$\frac{\mathrm{d}^2\hat{E}_R}{\mathrm{d}\zeta^2} + \left(1 + \frac{\eta}{\xi - i\gamma}\right)\hat{E}_R = 0$$

$$\eta = \frac{\omega_{pe}^2}{\omega^2} \propto n_e$$

$$\xi = \frac{\omega_{ce}}{\omega} - 1 = f(B_{z0})$$

1D

$$\boldsymbol{E}(t,\boldsymbol{x}) = \tilde{\boldsymbol{E}}\exp(-i\omega t + i\boldsymbol{k}\cdot\boldsymbol{x})$$

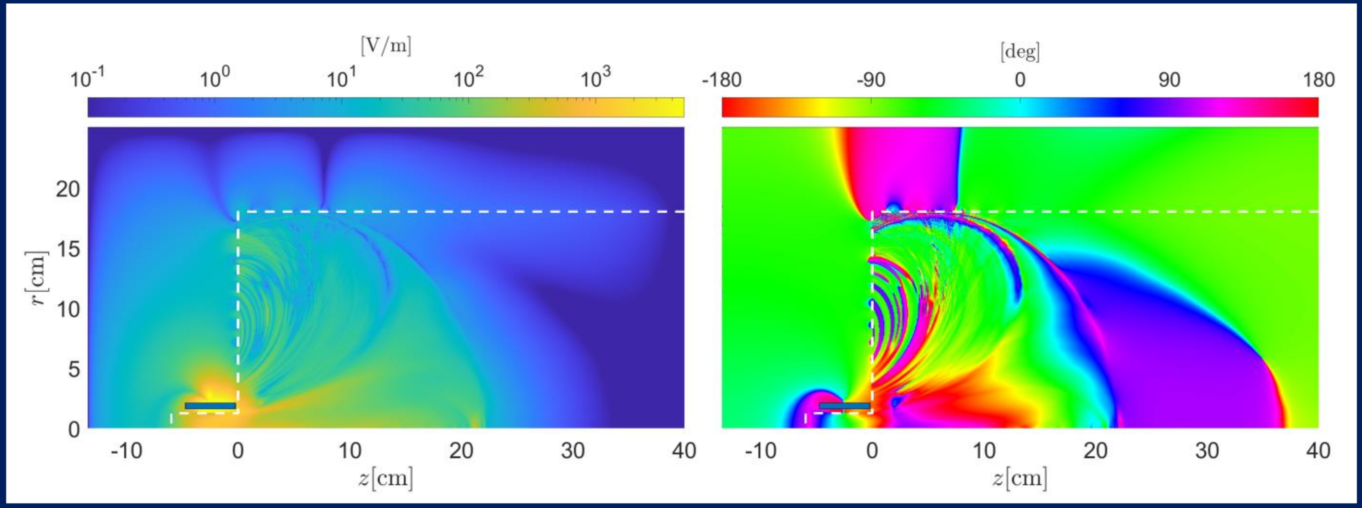

$$\nabla\times(\nabla\times\hat{\boldsymbol{E}}) - k_0^2\overline{\overline{\kappa}}\cdot\hat{\boldsymbol{E}} = i\omega\mu_0\hat{\boldsymbol{J}}_{\boldsymbol{a}},$$

$$S \equiv \frac{1}{2}(R+L) \qquad P \equiv 1 - \sum_s \frac{\omega_{ps}^2}{\omega(\omega + i\nu_m)}$$

$$D \equiv \frac{1}{2}(R-L) \qquad R \equiv 1 - \sum_s \frac{\omega_{ps}^2}{\omega(\omega + i\nu_m + \omega_{cs})}$$

$$\overline{\overline{\kappa}} = \begin{pmatrix} S & -iD & 0 \\ iD & S & 0 \\ 0 & 0 & P \end{pmatrix} \qquad L \equiv 1 - \sum_s \frac{\omega_{ps}^2}{\omega(\omega + i\nu_m - \omega_{cs})}$$

Implicit PIC Algorithm

- Compared to explicit PIC models:
  - $\Delta x > \lambda_{Debye}$ (no finite-grid instability $\longrightarrow$ enforces a minimum spatial resolution)
  - $\omega_{pe}\Delta t > 1$ (no CFL-type instability $\longrightarrow$ enforces a minimum temporal resolution)

- Basic implicit scheme based on Chen et al. 2011
  - The evolution of the particles is a function of the potential; non-linear elimination of the particle coordinates (**Particle enslavement**)

$$x_p^{n+1} = x_p[\Phi^{n+1}]; \qquad v_p^{n+1} = v_p[\Phi^{n+1}]$$

$$G\left(x_p^{n+1}, v_p^{n+1}, \Phi^{n+1}\right) = G\left(x[\Phi^{n+1}], v[\Phi^{n+1}], \Phi^{n+1}\right) = \tilde{G}\left(\Phi^{n+1}\right)$$

  - The residual is only a function of the potential
    - Major reduction of the non-linear system unknowns

- Fully Implicit Crank Nicolson mover
  - Time centered, 2nd order, non-dissipative

- Jacobian Free Newton Krylov (JFNK)
  - No need to compute the Jacobian Matrix
  - Jacobian vector product for Krylov subspace method (GMRES)
  - Easily preconditioned -> Potential for acceleration

SUBCYCLING AND MESH MAP

- In MN problems of interest,
  - Fields vary slowly (Δt).
  - Electron times are much faster ($\Delta\tau \ll \Delta t$).
  - Use small substeps such that $\sum \Delta\tau = \Delta t$.

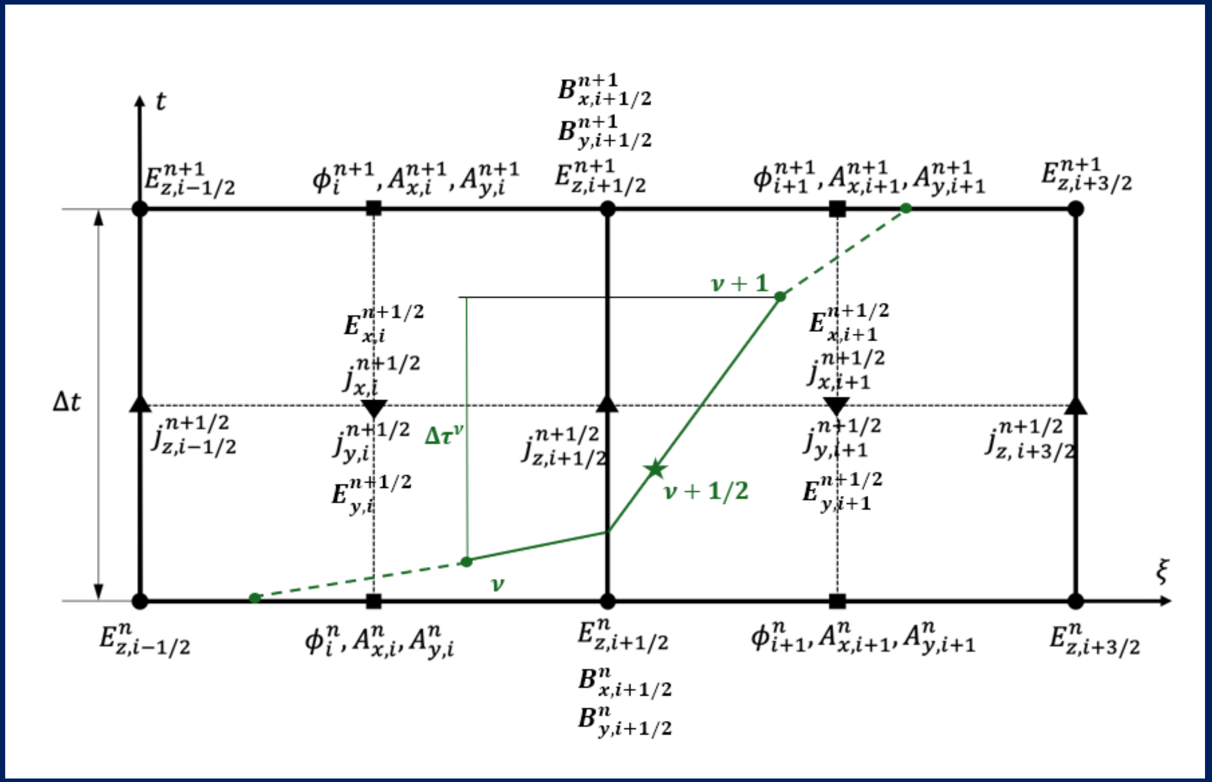

- Hybrid push in mapped meshes:
  - Particle positions are advanced in a Cartesian logical (computational) space and velocity advanced in physical space.

- Mover:
  - Particles are allowed to cross several cells in a substep -> Averaged splines.

- Conservation properties and stability:
  - Global energy → limits artificial heating.
  - Local charge $\partial_t \rho = -\nabla \cdot \boldsymbol{j}$ → important for long term sims.
  - Proven suppression of finite grid-instabilities under most conditions (Barnes 2020).

RECAP: ELECTROSTATIC STUDY

Jiménez, P., Chacón, L., & Merino, M. (2024). An implicit, conservative electrostatic particle-in-cell algorithm for paraxial magnetic nozzles. *Journal of Computational Physics*, 112826.

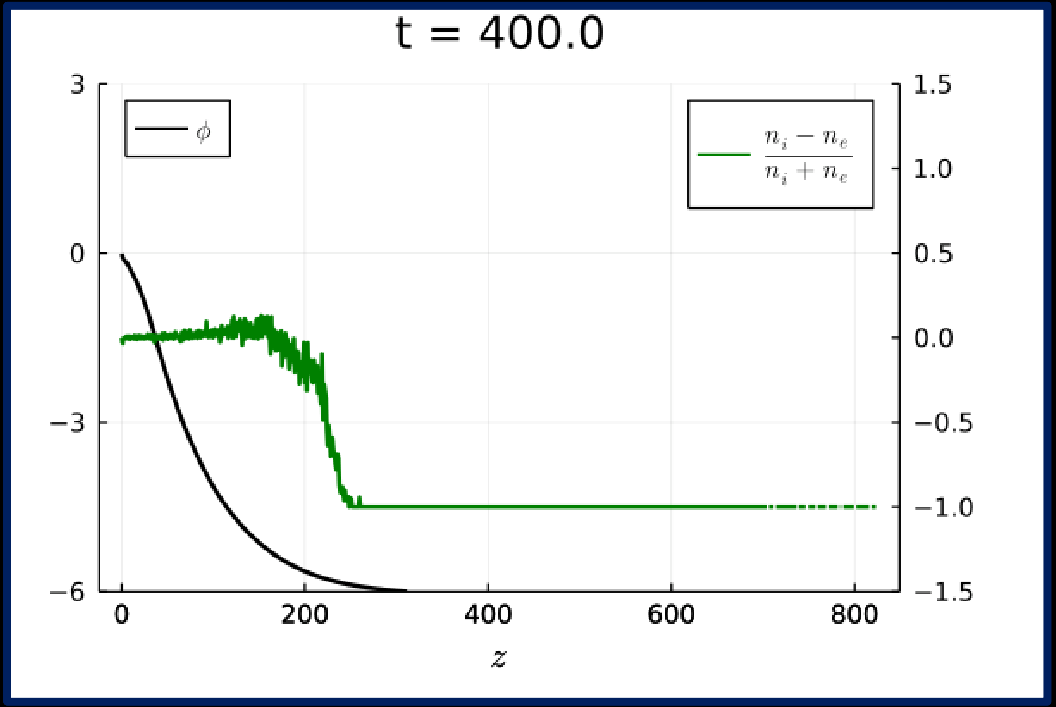

- 1D1V, electrostatic energy- and charge-conserving:
  - Conservation of μ.
  - Good agreement with previous literature.
  - Advances:
    - New downstream boundary conditions and elimination of the exit sheath.
    - Introduction of the segment-based mover in mapped meshes..

ELECTROMAGNETIC SIMULATION SETUP

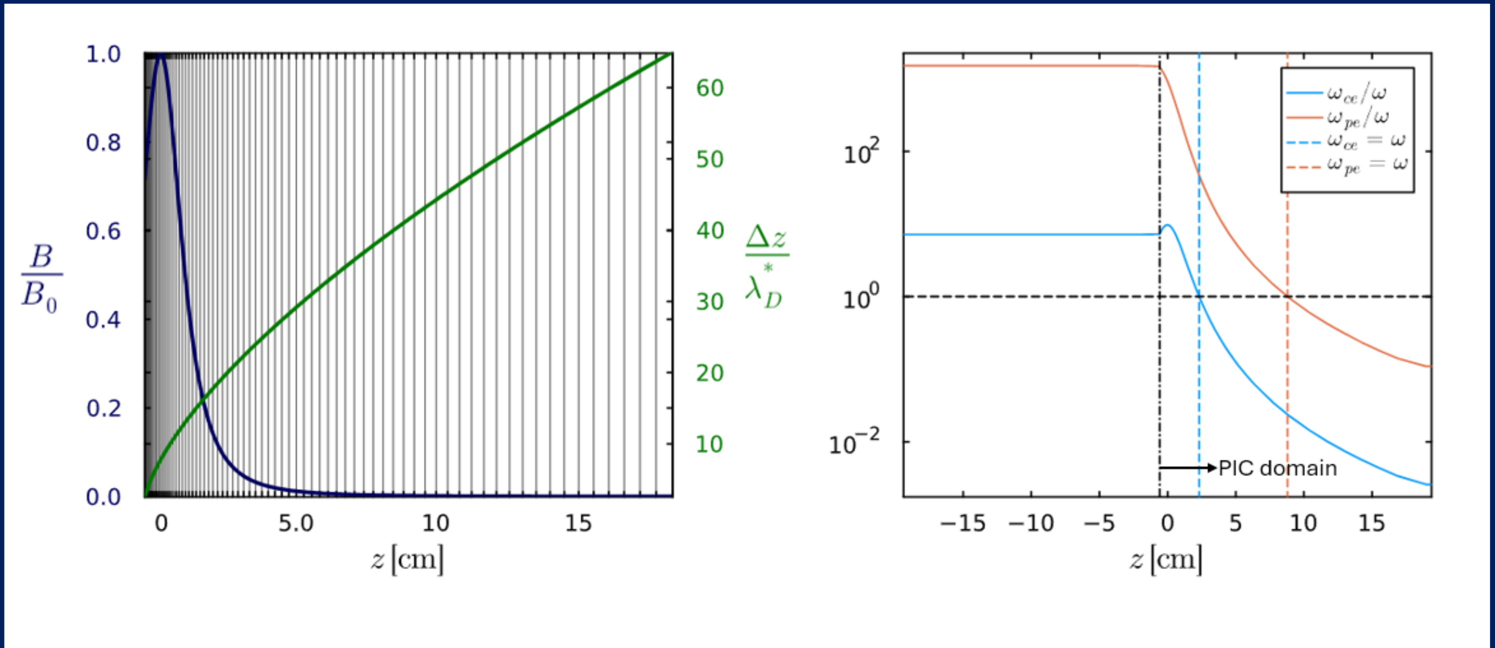

- Simplifications in preliminary simulations:
  - Reduced mass-ratio, lower ion transient time:
    - $\frac{m_i}{m_e} = 100$
  - Collision-less expansion.
  - Future work plans using realistic values.

- Plasma conditions close to typical EPT plume:
  - Convergent-divergent nozzle
  - Domain ~ 0.5 m
  - Density $\mathrm{n}_e = 10^{18}\ m^{-3}$
  - Electron temperature $T_e = 10\ eV$
  - Wave frequency $f = 260\ MHz$
  - Presence of an electron cyclotron resonance surface.

- Simulation cases:
  - **ES:** Electrostatic (i.e, no wave).
  - **EM:** Darwin, self-consistent wave simulation. Low and high-power cases.
  - **IW**: wave fields precomputed from cold-plasma dielectric tensor model.

STEADY STATE RESULTS: ELECTRON TEMPERATURE

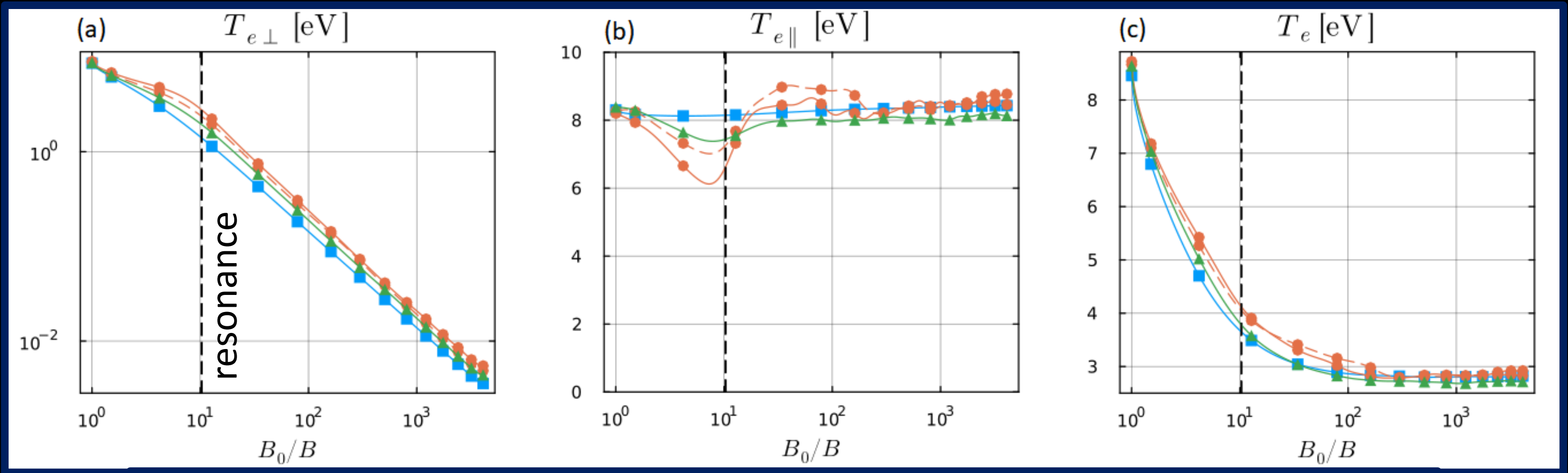

cases ES (■), EM.low (▲), EM.high (● solid) and IW (● dash).

- Electron perpendicular temperature $T_{e\perp}$
  - ES case: Decreases with 1/B as expected from magnetic moment μ conservation.
  - EM and IW: There is a broad heating region prior the resonance, higher $T_{e\perp}$ continues downstream.
  - Despite imposing the same approximate wave power, more heating is observed in EM.high than in IW.
- Electron parallel temperature $T_{e||}$
  - Almost constant in ES. Mirror force converts perpendicular energy to axial directed velocity.
  - Drop and recovery around resonance in EM and IW cases. Not well understood.
    - Possible particle synchronization, different subpopulation characteristics …

STEADY STATE RESULTS: POTENTIAL AND ION ACCELERATION

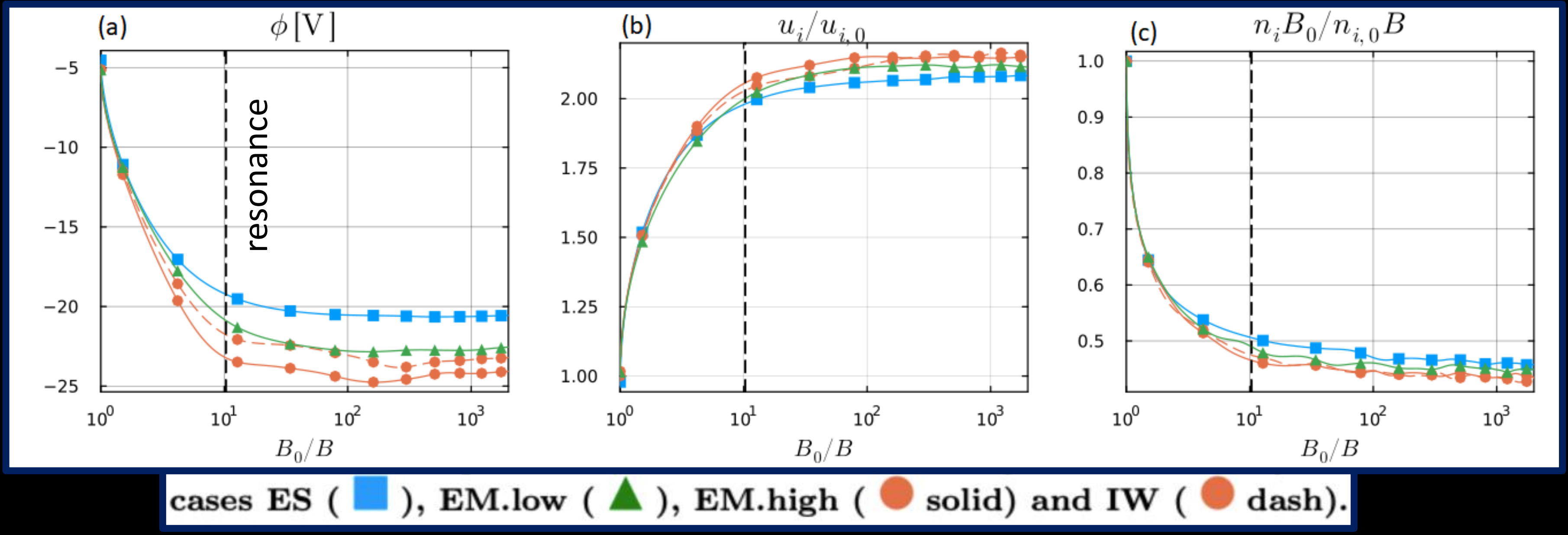

- Electrostatic potential
  - Larger fall in EM and IW thanks to the larger $T_{e\perp}$.
- Ion velocity:
  - Greater acceleration in electromagnetic cases $u_i \propto \sqrt{-\phi}$
  - Power transfer mediated by mirror force $\uparrow T_{e\perp} \rightarrow \uparrow v_{e,\parallel} \rightarrow \downarrow \phi \rightarrow \uparrow u_i$
- Fastest expansion:
  - Ion continuity $n_i A_{ft} u_i = n_i u_i / B$

Power deposition due to wave ultimately drives a higher thrust $F \sim m_i n_i u_i^2 / B$.

EM Fields and Power Absorption

- Wavefields propagate up to the resonance, where large absorption takes place
- Kinetic results were used to tune damping ratio γ of cold-plasma model
  - γ controls mainly the width of the absorption region.
  - In this case with <u>kinetic damping</u> only: $\gamma \simeq 0.5\omega$ offers a good fit
- Minor differences in phase and magnitude between EM and IW cases.
  - Simple fits could be derived over a range of problems of interest

Weighted from particles (not the one in cold-plasma model).

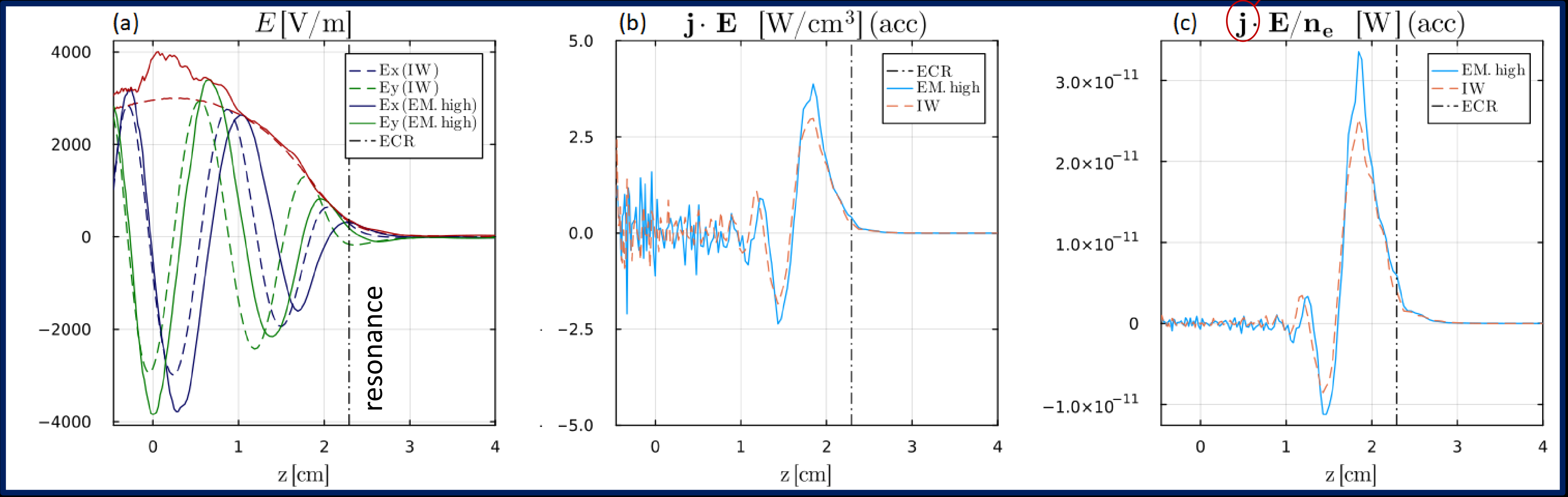

The magnetic moment μ is not conserved in the heating region. Downstream the resonance the typical trend resumes.

Near-vertical lines in the gyro-phase suggest particle synchronization with wave fields in EM and IW cases.

A structure in v_z appear that coincides with a displaced resonance line due the Doppler effect on hot particles:

$$\omega_{eff} = \omega_{ce}; \qquad \omega_{eff} = \omega - v_t k$$

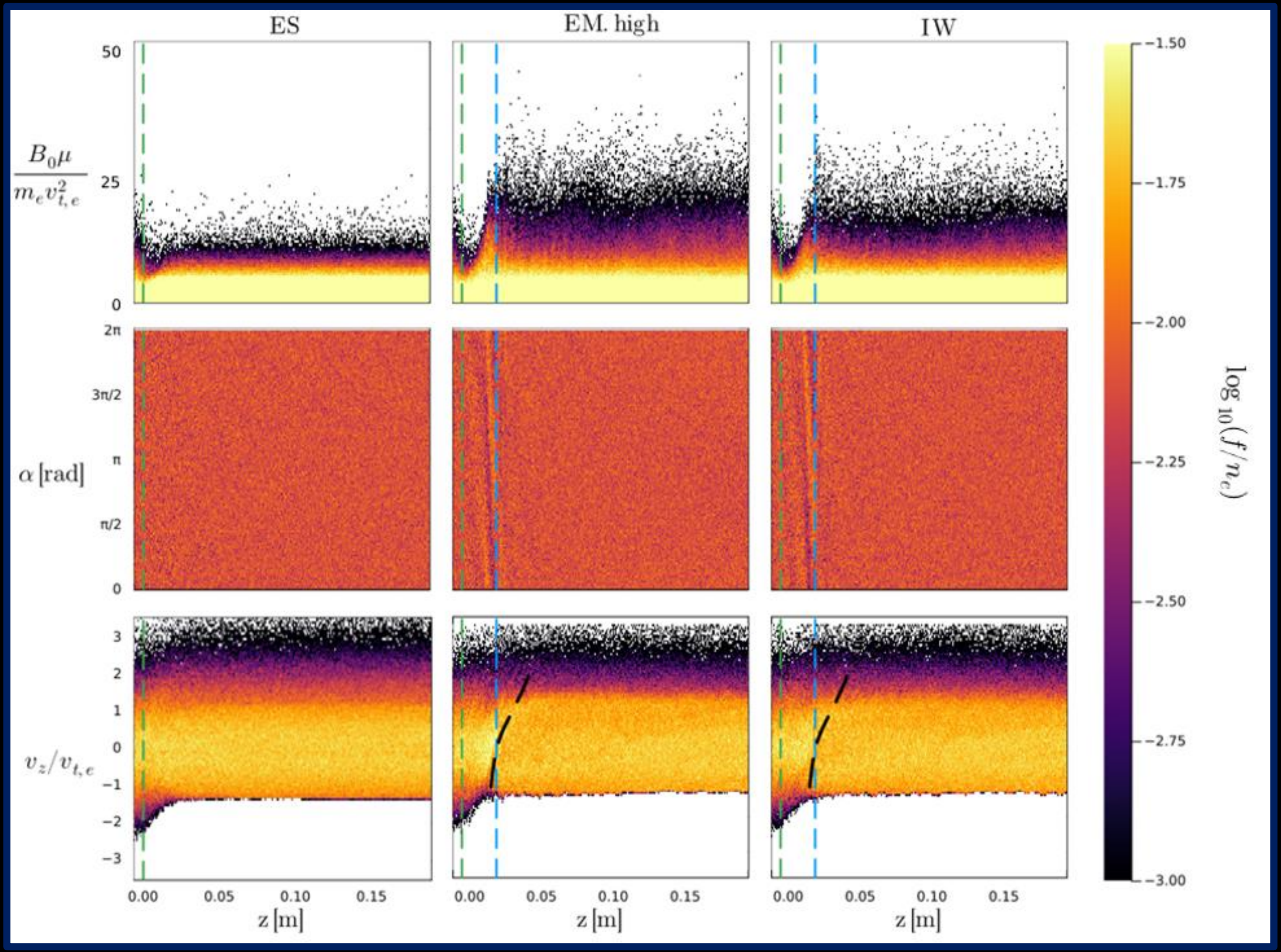

Algorithm Performance Electrostatic

- Realistic mass ratio simulations ~ 1 day 20 core workstation.
- Linear time scaling with particles/cell and number of cells.
- $t_{tot} \propto n_z$ → New mover allows particles to travel across several.
- Speed up of $O(10)$ with respect to explicit PIC: For typical mesh and timesteps.

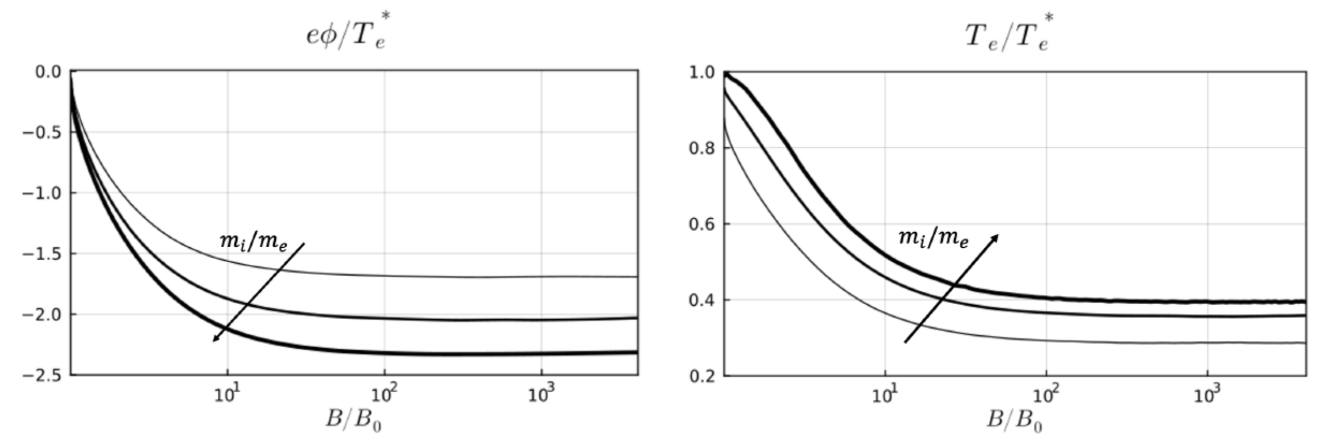

Figure 6.10: Steady-state potential (left) and total temperature $T_e = (2T_{\perp e} + T_{\parallel e})/3$ (right) for case B ($m_i/m_e = 100$), H^+ ($m_i/m_e = 1836$), and Xe^+ ($m_i/m_e \sim 240000$).

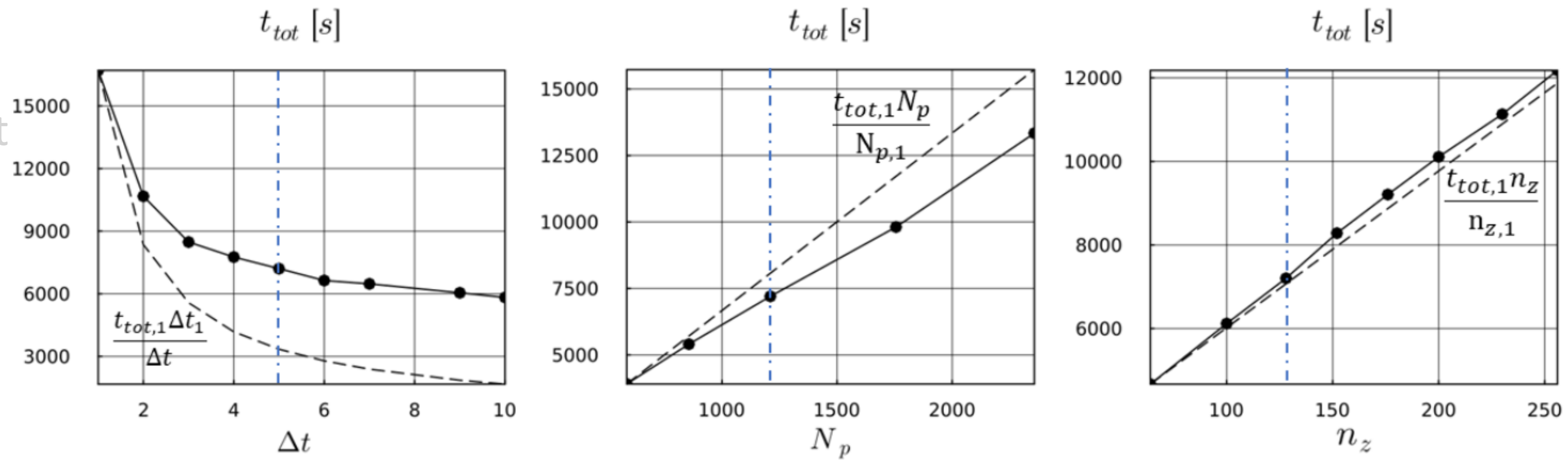

CONCLUSIONS AND FUTURE WORK

- Time-implicit → breaks λ_{De} and ω_{pe} constraints. Darwin model to avoid solving fast light speed modes.
- Exact global-energy and local-charge conservation.
- Good agreement between Darwin and cold-plasma model:
  - Fitting of phenomenological parameters with self-consistent simulations.
- Important performance gain compared to state-of-the-art:
  - Greater than in electrostatic studies.
  - Challenges: Convergence (preconditioning), population control …

$$\frac{CPU_{exp}}{CPU_{imp}} \sim \frac{0.01}{(k\lambda_D)^d}\frac{c}{v_A}\min\left[\frac{1}{k\lambda_D}, \frac{c}{v_A}\sqrt{\frac{m_e}{m_i}}, \sqrt{\frac{m_i}{m_e}}\right]\frac{1}{N_{FE}}$$

- Back-of-the envelope estimate (Chen 14) with EPT plasma:

  1D -> O(100)

  2D -> O(2500)

  3D -> O(60000)

- Future work:
  - Implement preconditioner
  - Adding MC collisions
  - 2D dimensional code
  - GPU parallelization

- Possible IPIC Applications in Electric Propulsion:
  - Nozzles and expansions.
  - Plasma sources.
    - Need for collisions, plasma chemistry and wall interaction.
  - Electrodeless Thrusters (EM version).

ACKNOWLEDGMENTS

The work of Pedro Jimenez and Mario Merino has received funding from the European Research Council (ERC) under the European Union’s Horizon 2020 research and innovation program (grant agreement No 950466)

Thank you!

Questions?

pejimene@ing.uc3m.es

ZARATHUSTRA